



## Green Synthesis of Graphite Oxide as Metal Free Catalyst for Petrochemicals Production

Aya M. Matloob<sup>1</sup>, Dalia R. Abd El-Hafiz<sup>1</sup>, L.Saad<sup>1</sup>, S.Mikhail<sup>1</sup>, D.Guirguis<sup>2</sup>

<sup>1</sup> Egyptian petroleum research institute, <sup>2</sup> Ain Shams University.

### Abstract

Graphite oxide was synthesized by the modified Hummer's method.

The degree of the oxidation of the graphite was systematically controlled via the oxidation time,  $\text{KMnO}_4$  : Graphite wt. ratio and the addition of the phosphoric acid to the oxidation media. The Physicochemical properties of the synthesized graphite oxide are investigated by using different techniques ; XRD, FTIR, zeta potential, and TEM. It was found that the structure of the expanded graphite can be easily and remarkably disordered by oxidation. Three phases of interlayer distances were identified at 3.4 , 4 and  $6\text{\AA}$  , specified for the pristine graphite, intermediate and the fully expanded graphite oxide respectively . These phases were corresponding to the compositions : epoxide, carboxyl and hydroxyl groups respectively . as confirmed by FTIR.

The catalytic activity of the prepared graphite oxide samples was tested for petrochemical production from the ethanol conversion reaction at different reaction temperature 100-250°C and resulted pressure ranging 40-92 atm . The converted products were mainly composed of acetone, ethylene, acetaldehyde, diethylether, and heavyhydrocarbons( >c). Acetone was found to be the main product at all reaction temperatures with selectivity "53-94%". XRD and TEM analyses of the prepared samples confirmed the transformation of the prepared graphite oxide into graphene like material at reaction temperature 250°C.

**Keywords:** Graphite; Graphite Oxide; Graphene; Ethanol Redox Reaction .

### 1. Introduction

Carbon nano structures have been extensively studied due to their excellent properties and numerous applications [1]. The structure and the surface property of the carbon nanostructures have been extensively studied, little attention has been paid to the chemical reactivity especially when used as catalysts. Coughlin [2]classified carbon catalysts into three categories according to their electrical conductivity; conductors, semiconductors, and insulators. The insulator carbon can catalyze different reactions such as isomerization, cracking, dehydration, polymerization and so on.

Graphite oxide (GO) is an interesting class of carbonaceous material due to its special surface properties and layered structure [3-5]. It is a non-stoichiometric material with chemical composition written as  $\text{C}_x^+(\text{OH})_y^-(\text{H}_2\text{O})_z$ , it has strong covalent bonding along the basal planes with weak hydrogen-bonded intercalated water molecules in the interlayer spacings [6], It's surface comprises different oxygen-containing groups such as C-OH, -COOH and epoxide, which confer an acidic character to the material "GO" function as Bronsted acid sites.

However, it is important to control the acidity of the prepared material to use as catalysts in certain reaction, which can be achieved by changing the condition in GO synthesis. Many experiments were performed using different oxidation treatment times varied from 24 hrs to longer[7]. Since the graphite oxide obtained after 24 hrs or more of oxidation is fully insulated with light brown colours. A more intriguing oxidation time is less than 24 hrs, in which graphite oxide can be turned from an insulator to a semiconductor with different band gaps.

**The aim of this work deals with three folds :**

- ii) Controlling the synthesis parameters (oxidation time, Graphite/KMnO<sub>4</sub> wt.ratio, addition of H<sub>3</sub>PO<sub>4</sub>) on the oxidation level of graphite ,
- iii) Investigating the effects of the oxidation level on the physical and chemical properties such as the interlayer distance and variable detectable functional groups of the prepared graphite oxide by using different analytical technique,.....and
- iiii) Examining the activity of the prepared graphite oxide as a catalyst in ethanol conversion into valuable petrochemical products.

## 2. Experimental

### 2.1. Preparation of Graphite Oxide

Graphite oxide was prepared by the improved hummer method [8]. 3gm of graphite powder was added to 70 ml concentrated H<sub>2</sub>SO<sub>4</sub> (98%) and 6.7 ml phosphoric acid (85%), under stirring in an ice bath for 30 min. After that, an appropriate amount of KMnO<sub>4</sub> based on the amount of the graphite powder (with wt.ratio 1:1, 2:1 & 3:1) was slowly added under vigorous agitation. The mixture was stirred for different times (6, 12 & 24 hrs) at room temperature. A dark green suspension which turned to highly viscous mixture as the time increased, was formed due to oxidation of the graphite and the formation of the precipitated MnO<sub>2</sub>[9]. To quench the oxidation reaction, 500ml distilled water was added to the mixture under vigorous stirring for 15min at reaction temperature 95°C, followed by slow addition of 15ml H<sub>2</sub>O<sub>2</sub> until the color turned from dark brown to yellowish due to the reduction of the residual permanganate and the precipitated manganese dioxide to colorless soluble manganese sulfate [10]. The mixture was allowed to stand for at least 12 hours, then the clear supernatant was decanted and the remaining precipitate was washed with hot distilled water. The obtained graphite oxide was dried at room temperature (the color of graphite oxide become metallic gray).

### 2.2. Characterization of the Prepared Samples

The structural characterization of the prepared samples have been studied by different techniques.

#### 2.2.1 X-ray Diffraction Analysis (XRD)

X-ray diffraction analysis was carried out by Shimadzu XD-1 diffractometer using Cu-target and Ni-filtered radiation, to trace the various changes in the crystalline structure and the different phases accompanied preparation method. Sample powders were packed in a glass holder, and then measurements were taken of the diffraction intensity by step scanning in a 2θ range between 5° and 70°. The phase identification was made by comparison with the Joint Committee on Powder Diffraction Standards (JCPDS).

#### 2.2.2 Fourier Transform Infrared Spectroscopy (FTIR)

Fourier transform infrared spectroscopy was used to characterize the main constituents of the prepared samples. Analysis was carried out using ATI Mattson 1001 in the wave number region of 400-4000cm<sup>-1</sup>. All samples were ground with potassium bromide (KBr) powder and then pressed into a disk before analysis.

#### 2.2.3 Transmission Electron Microscopy (TEM)

Transmission electron microscopy was conducted using a JEOL 2100F TEM at an accelerating voltage of 200 kV. TEM was used to study the morphology and the size of the prepared samples. To prepare the TEM samples, a dilute particle-ethanol colloidal mixture was ultrasonicated for 30 min and a drop of the solution was placed on a carbon coated Cu TEM grid.

### 2.3. Catalytic Activity

The catalytic activity of the prepared graphite oxide is carried out by using PID autoclave 316 stainless steel reactor, with an inner volume of 300ml, at different reaction temperature (100-250°C) and accompanying pressure (40-90 atm). 5 gm graphite oxide sample dispersed in 100 ml absolute ethanol was introduced into the autoclave. Then the reactor being tightly sealed, the temperature and the pressure were raised to the required ones and at the reaction time of two hours.

At the end of the run, the reaction was quenched immediately by passing a cold water in the coil inside the reactor. the gaseous product was collected, and the suspended reactant was filtered to get the liquid products.

The gas chromatography was used to analysis the gaseous and liquid product using (Agilent 6890 plus HP) equipped with a capillary column (HP-1 dimethylpolysiloxane, 60 meters in length, 0.32 mm in internal diameter and 0.5mm film thickness) using a flame ionization detector (FID) with N<sub>2</sub> as the carrier. The temperature of the injector and detector was set at 250°C & 300°C respectively. The temperature program of the oven was 50°C (hold 3min) ramped 3°C/min until 220°C (hold 15min). The carrier flow rate was constant (2ml/min). The data analysis of the peak area was normalized

using software chemstation and external standard (to identify retention time and response factor for each component) for the calculation of the product %.

### 3. Results and Discussion

#### 3.1 Characterization of The Prepared Graphite Oxide Samples

##### 3.1.1 X-ray Diffraction

The parent graphite and the prepared graphite oxide samples are subjected to X-ray analysis. The information concerning the crystalline phases of the prepared graphite oxide samples together with their characteristic d-spacing ( $\text{\AA}$ ), their relative intensities and their confirmed JCPDS cards are represented in Fig. (1).

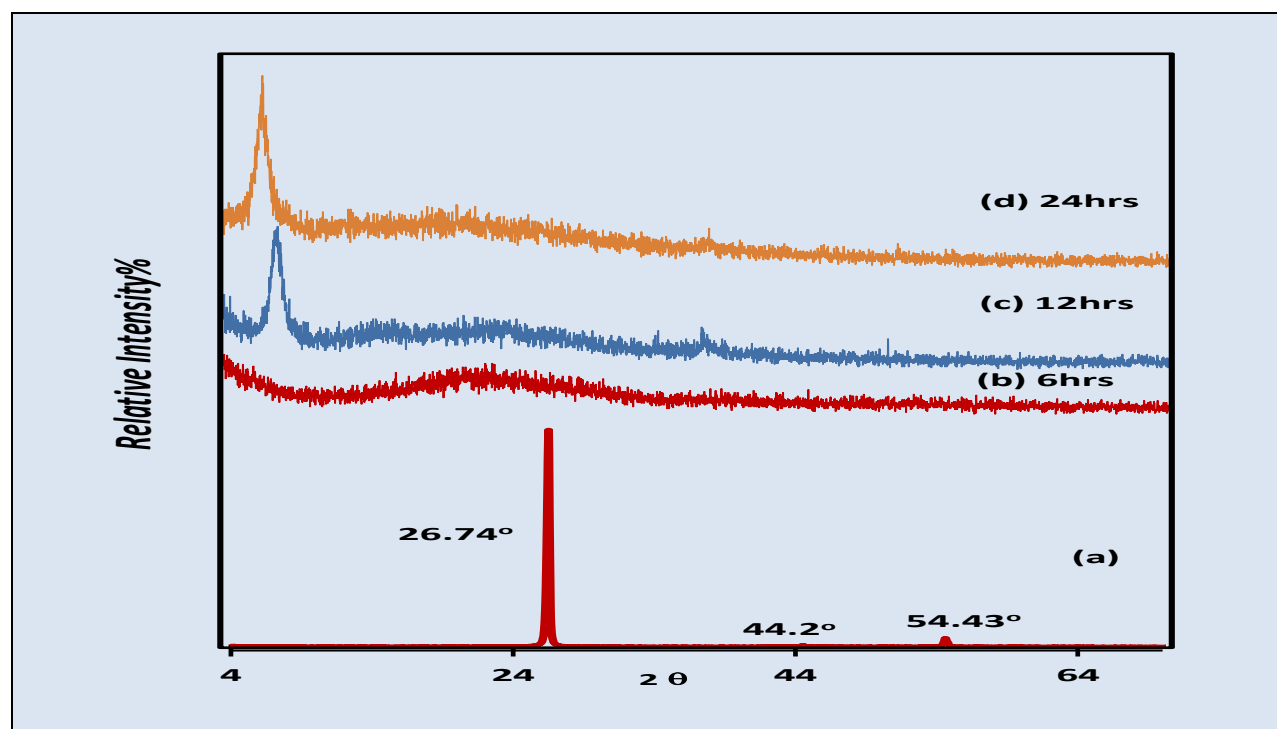
X-ray diffraction pattern of the parent graphite (Fig. 1a) indicates the appearance of a very sharp peak at  $2\theta = 26^\circ$  corresponding to (002) plane with an interlayer distance of  $3.34 \pm 0.005 \text{\AA}$ , in addition to small peaks at  $2\theta = 44^\circ$  &  $54.43^\circ$  corresponding to the interlayer distances of  $1.079 \pm 0.005 \text{\AA}$ , and  $0.81 \pm 0.005 \text{\AA}$ , respectively (JCPDS card NO.75-1621).

For the graphite oxide samples, different phases of interlayer distances were identified during the oxidation of the parent graphite powder (Fig. 1.b-d). XRD pattern for the sample oxidized for 6hrs (fig 1.b). shows only an intermediate phase (water like Graphite) at  $2\theta \sim 24^\circ$  which attributed to the hydroxyl groups that converted to the epoxide and carboxyl groups as the oxidation time progressed, enhancing the interlayer distance and switching the carbon backbone to a  $sp^3$  structure in agreement with Szabo et al'fact [11].

XRD patterns (fig. 1-b-d) reveal that the intermediate phase appeared at  $\sim 24^\circ$ , disappeared as the oxidation time increases from 6 to 12 then 24hrs. At the same time a new high intensity sharp peak appeared at  $2\theta \sim 8^\circ$  corresponding to an oxygen-related peak  $6.08^\circ$  in which the interlayer distance increases up to  $6.08 \text{\AA}$  &  $6.7 \text{\AA}$  for the samples oxidized for 12 & 24hrs respectively; due to the formation of the graphite oxide phase.

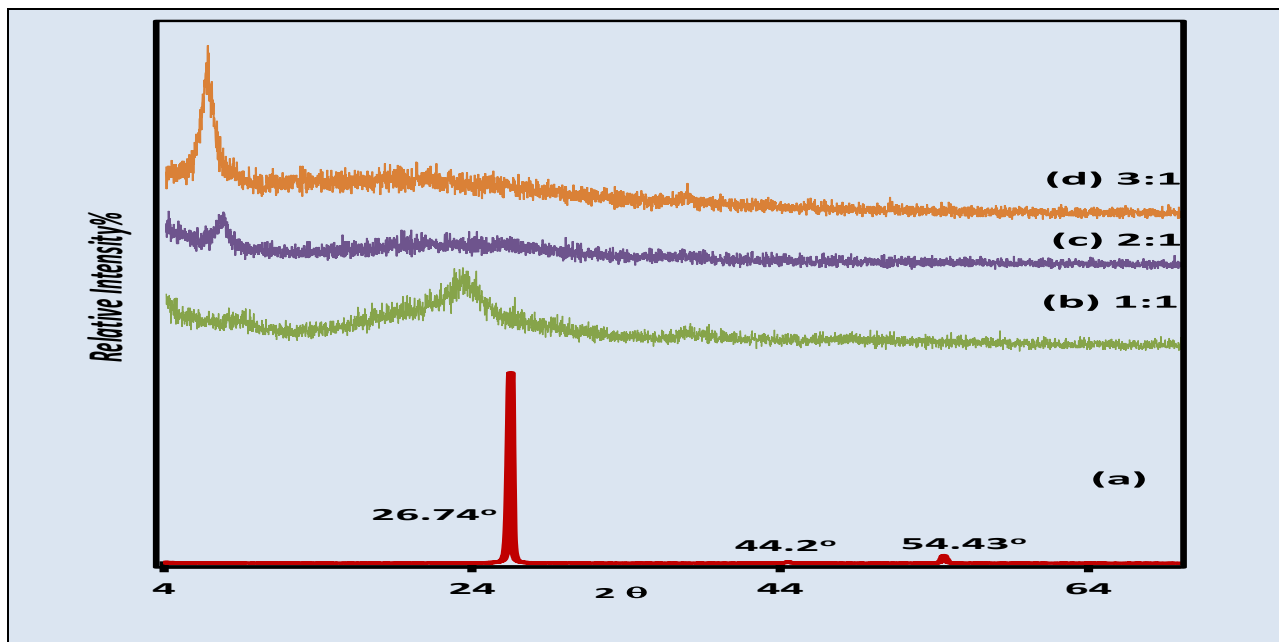
Another small peak at  $2\theta \sim 44^\circ$  is observed for all graphite oxide samples showed the (100) in-plane phase indicating a lattice constant of  $1.4 \text{\AA}$  in the plane [12]. Therefore, graphite oxide retained a lattice constant similar to that of the parent graphite, which insures that the graphitic structure of the prepared graphite oxides are not distorted through the oxidation process [13].

Fig. (1): XRD Patterns of the Parent Graphite and the Prepared Graphite Oxide Samples at Different Oxidation Times



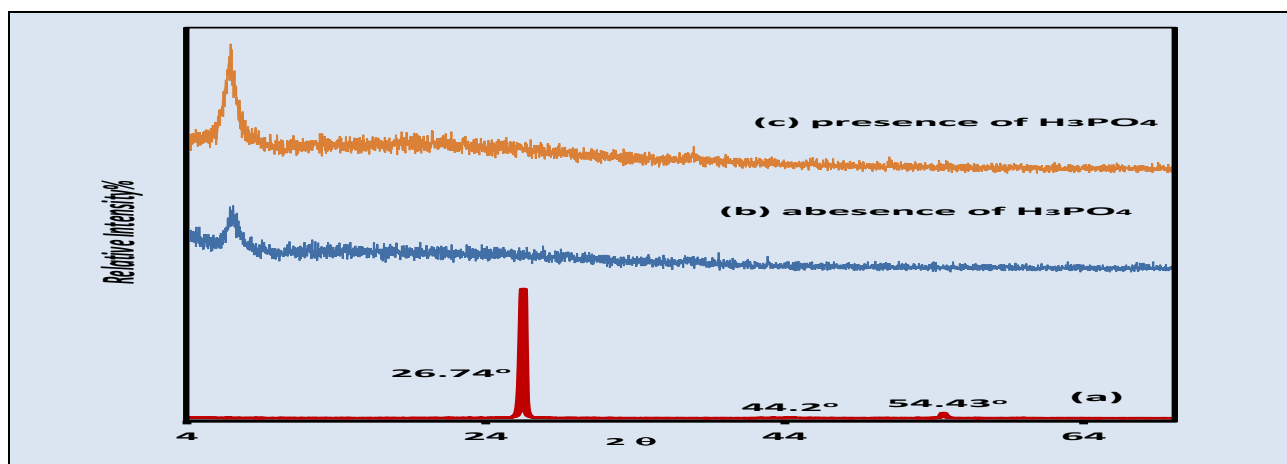
XRD patterns for graphite oxide samples prepared by changing KMnO<sub>4</sub>: graphite weight ratio (Fig. 2), show that, with the increase in KMnO<sub>4</sub>: Graphite wt. ratio from 1:1, to 2:1 then to 3:1, the graphite phase centering at 26.46° shifted to lower 2θ ~ 24° with broadening peak (water like phase). Besides, the appearance of a very small oxygen- related peak near 2θ 9° corresponding to d- spacing = 11.86Å is appeared that sharply increased, as the KMnO<sub>4</sub>: Graphite wt. increases from 2:1 ratio to 3:1. The expansion of the interlayer distance of GO samples is attributed to the generation of oxygen-containing groups and the presence of adsorbed water between the hydrophilic graphite oxide layers. Therefore, the higher Wt.ratio KMnO<sub>4</sub>: Graphite (3:1) is seemed to facilitate the intercalation and oxidation of graphite.

Fig. (2): XRD Patterns of the Parent Graphite and the Prepared Graphite Oxide Samples at Different KMnO<sub>4</sub>: Graphite Wt.Ratio



On the other hand, the effect of adding phosphoric acid during the oxidation processes is also studied for the prepared sample after an oxidation time=24 hrs and with KMnO<sub>4</sub>: graphite wt. ratio 3:1. The XRD patterns (fig.3) reveal that, the presence of phosphoric acid in the oxidation media enhances the oxidation process as indicated by the sharp and the significantly shifted GO line to the lower 2θ~7.2

Fig. (3): X-ray Diffraction Patterns of the Parent Graphite and the Prepared Graphite Oxide Samples Prepared in the Absence and Presence of H<sub>3</sub>PO<sub>4</sub>.



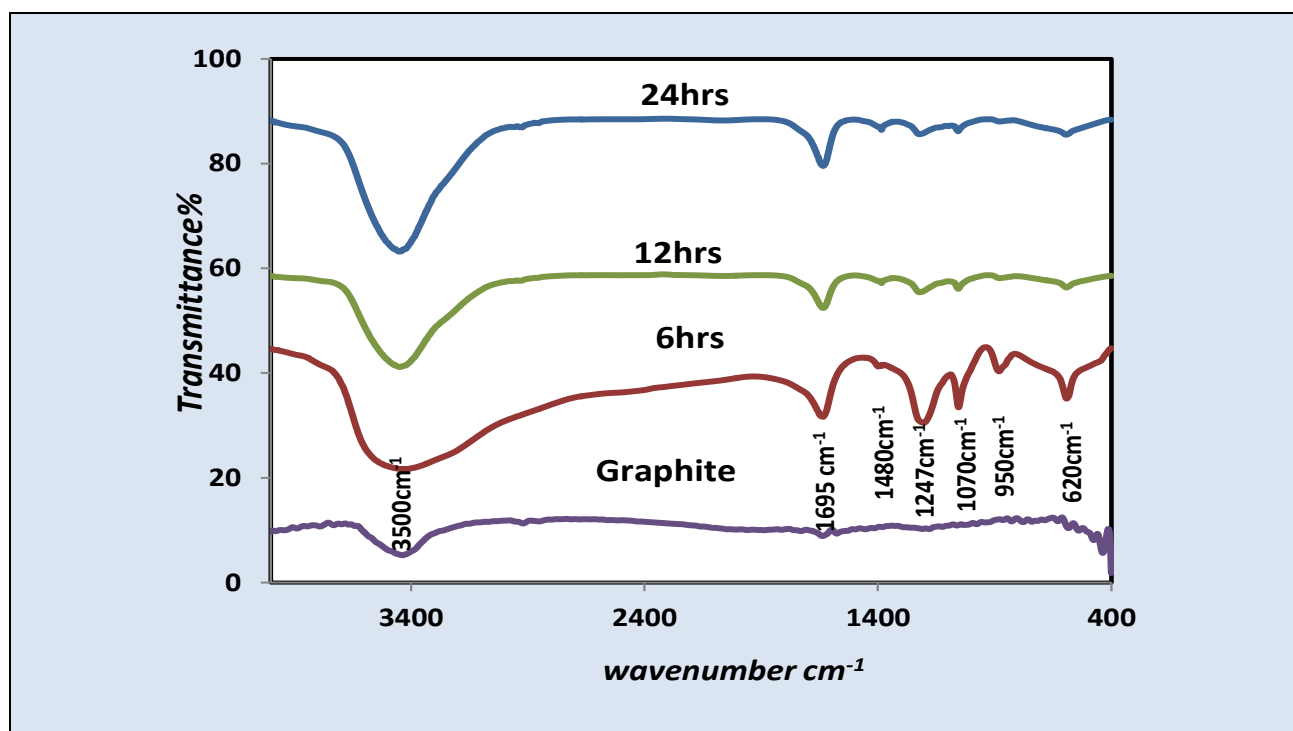
### 3.1.2 Fourier Transform Infrared Spectroscopy (FTIR)

FTIR spectrum of the parent graphite sample (Fig. 4-a), is like a flat line, the very weak transmission peaks present in this line may be due to the small impurities in the graphite powder. The spectra of the oxidized graphite samples (Fig.4-b-d), reveal the appearance of a broad band in the region between  $3000$  and  $3780\text{cm}^{-1}$  which is assigned to the free, associated hydroxyl groups and to the surface hydroxyl groups [14]. Upon oxidation the intensity of this band is increased with the increase in the oxidation time from 6 to 12 then 24hrs, which implies that the sample has the most saturation level after 24hrs (Fig. 4).

A detected band located at  $1695\text{cm}^{-1}$  with high intensity confirms the presence of either carboxylic acid and/or carbonyl group that also saturated by longer oxidation time. The appearance of the peaks at  $1247\text{cm}^{-1}$  is due to deformation vibration in C-OH and/or C-O stretching vibration of C-O-C.

On the other hand the appearance of the epoxide bands at  $1070\text{cm}^{-1}$  and  $969\text{cm}^{-1}$  for the sample at an oxidation time 6hrs and its disappearance with the longer oxidation time (12, 24hrs) [15], may be attributed to the instability of the epoxide bond.

Fig. 4: FTIR Spectra of the Parent Graphite and the Graphite Oxide Samples Prepared at Different Oxidation Time



As clarified from the above results the FTIR spectra (figs 5, 6) show that, as the  $\text{KMnO}_4$  : Graphite wt. ratio increases and in the presence of phosphoric acid (fig.6), the oxidation to graphite oxide increases. This finding is also consistent with the XRD data.

Fig. 5: FTIR Spectra Of The Parent Graphite And The Graphite Oxide Samples With Different Graphite:  $KMnO_4$  Ratio

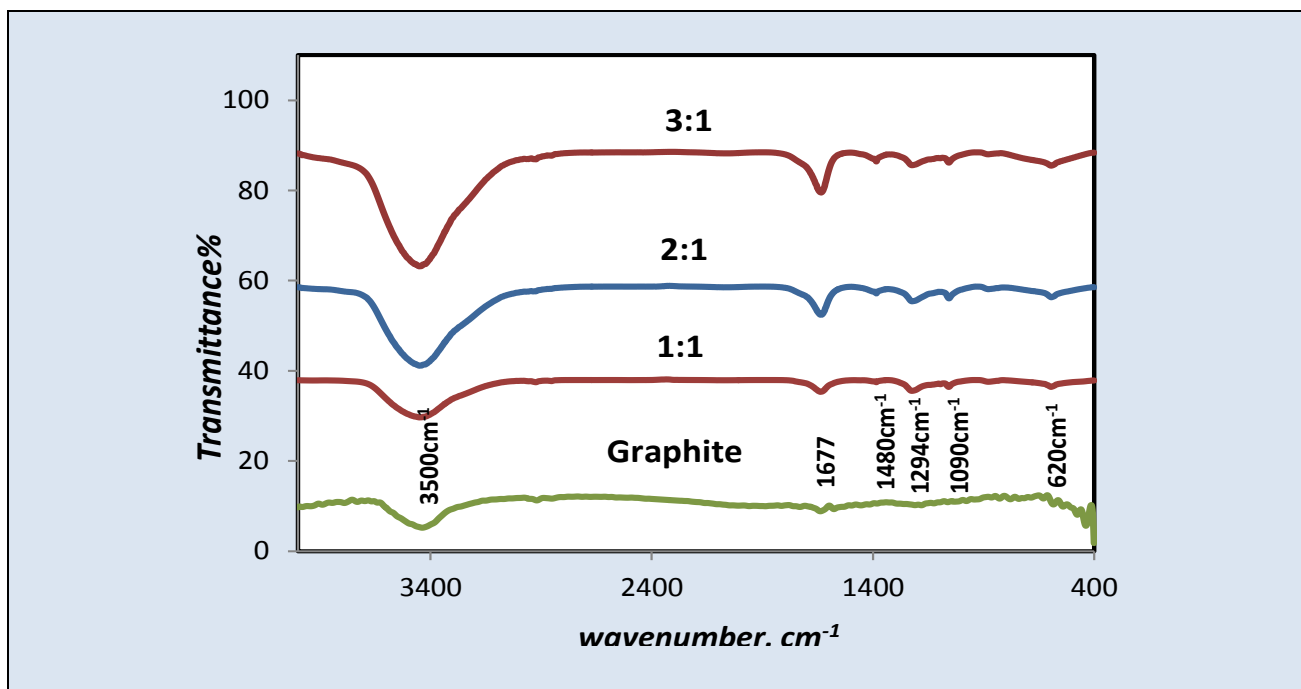
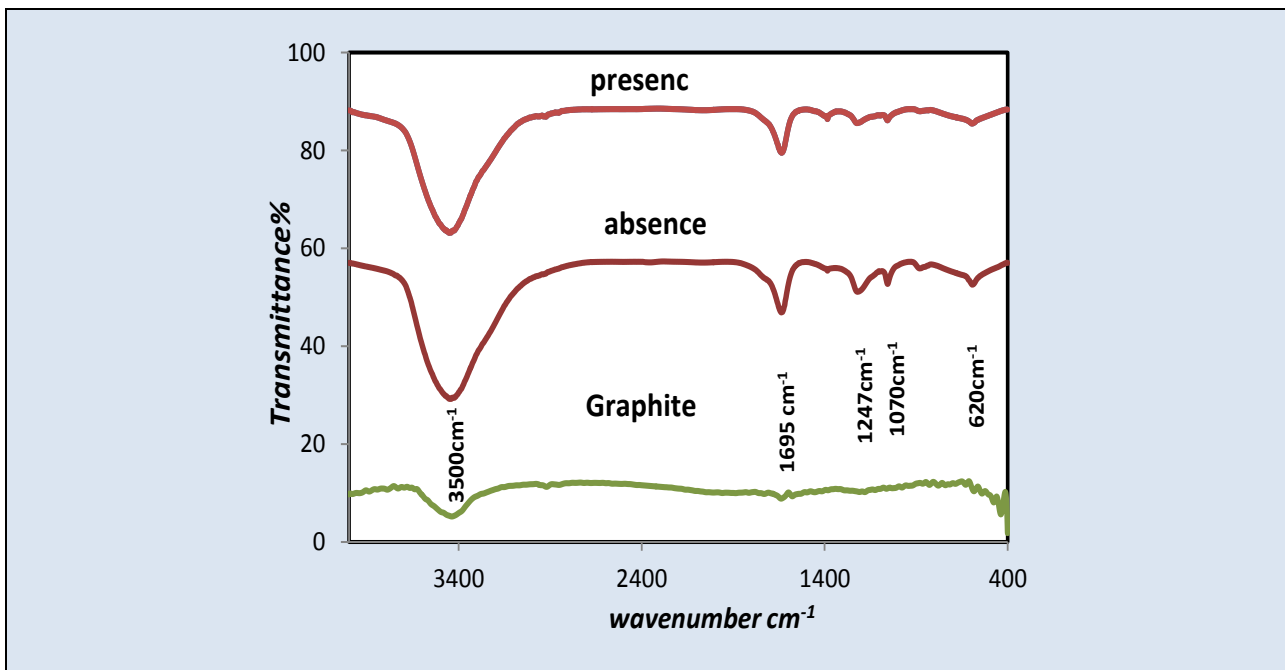


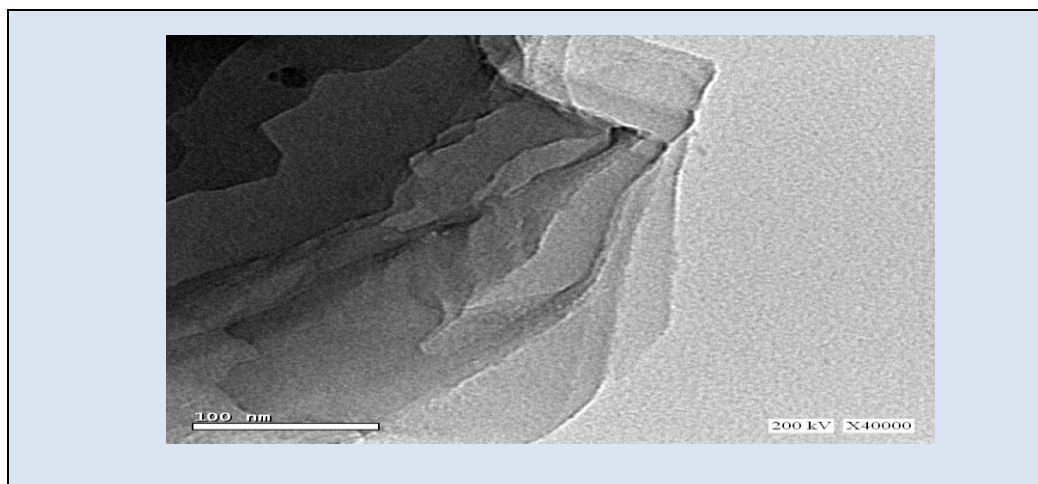
Fig. 6: FTIR Spectra of the Parent Graphite and the Graphite Oxide Samples Prepared in the Presence and Absence of Phosphoric Acid



### 3.1.3 Transmission Electron Microscopy (TEM)

The morphology of graphite oxide can be observed (Fig.7) . The sp<sup>3</sup>-bonded carbon atoms allocated in the graphene sheets disrupt very effectively the double bond conjugation and account for the waved sheet structures, resembling wrinkled silk, which is typical for GO .

**Fig.7: TEM Image of Graphite Oxide**



### 3.1.4 Zeta Potential

The stability of the prepared graphite oxide samples were checked via Zeta potential (ZP) measurements of the nanoparticles under suspension, using Zeta Sizer Nano equipment. Recall that ZP indicates the level of the repulsion between particles similarly charged in dispersion. Thus, the higher is the ZP, the more the dispersion, i.e, resist aggregation and a longer period of stability.

Zeta potentials ( $\zeta$ ) of aqueous dispersions, are all negative because of the ionization of the oxygen-containing groups . As shown (Table 1), the highly oxidized graphite sample with higher KMnO<sub>4</sub>:Graphite Wt. ratio has the lowest  $\zeta$  potentials values and hence more stable in aqueous dispersion, which is attributed to the increased oxidation degree, especially the increased carboxyl group concentration on GO.

**Table. 1: Zeta Potential (ZP) Measurements of the Prepared Graphite Oxide Samples**

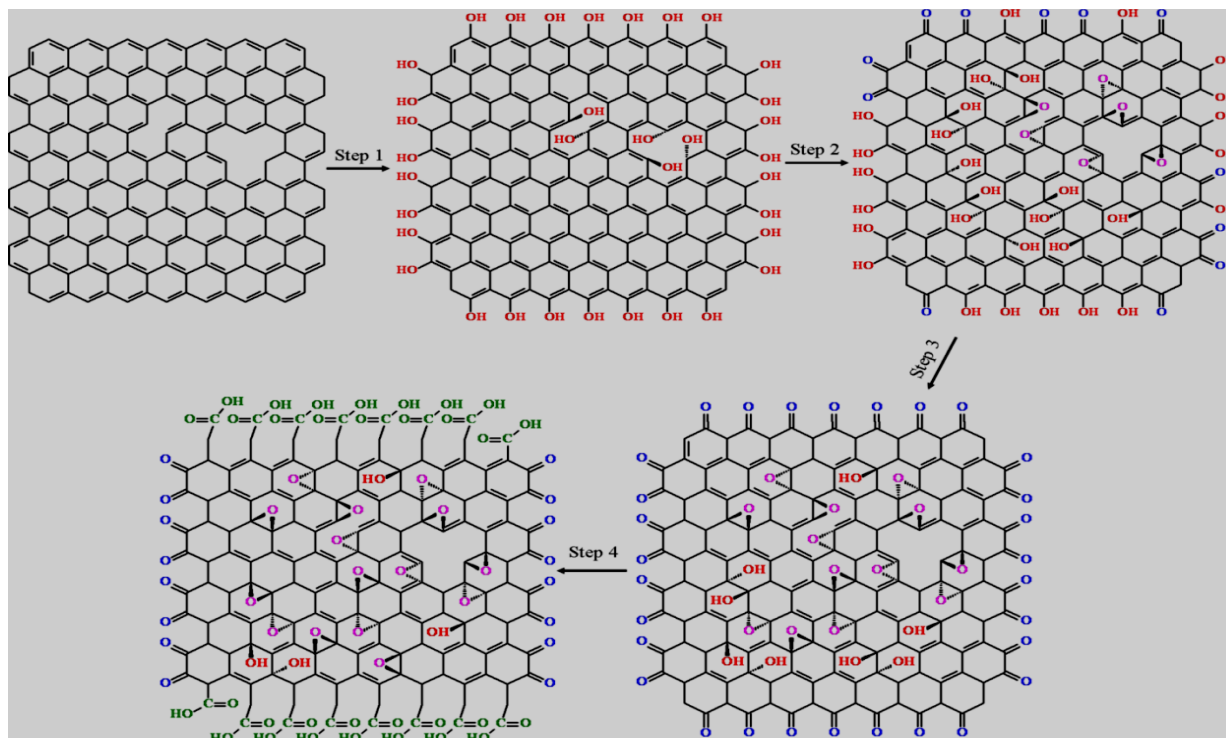
KmnO <sub>4</sub> :Graphite	Graphite Oxide Samples		
	Time Hrs	Effect of Phosphoric Acid	Zeta Potential (mv)
3:1	24	presence	-43.5
3:1	12	presence	-40.5
3:1	6	presence	-20.5
2:1	24	presence	-30.3
1:1	24	presence	-19.5
3:1	24	absence	-36.9

From the X-ray diffraction , Fourier transform infrared spectroscopy (FTIR) , TEM,and zeta potential data , it can be concluded that, the prepared graphite oxide consists of intact graphitic regions interspersed with sp<sup>3</sup> hybridized carbons



containing hydroxyl and epoxide functional groups on the top and bottom surfaces of the sheet and sp<sup>2</sup> hybridized carbon containing carbonyl and carboxyl functional groups mostly at the sheet edges as shown in Fig.8.

Fig.8: Mechanism of Formation Of Oxygen Containing Group of GO



### 3.2 Catalytic Activity

The oxidation–reduction reaction of ethanol was taken as a model reaction to study the catalytic activity of the prepared graphite oxide as an oxidant catalyst and to investigate the reduced graphite oxide material i.e., like graphene.

From the previous result the graphite oxide sample, prepared at 24hrs and with KMnO<sub>4</sub>: Graphite of 3:1 wt. ratio was selected to study the catalytic oxidation of ethanol at different reaction temperature (100–250°C), and under atmospheric pressure (14–95atm). The results are included in table (2) and graphically illustrated in (Fig.9).

Data in Fig.(9) clarifies the increase in the catalytic activity of the prepared graphite oxide with the increase in the reaction temperature.

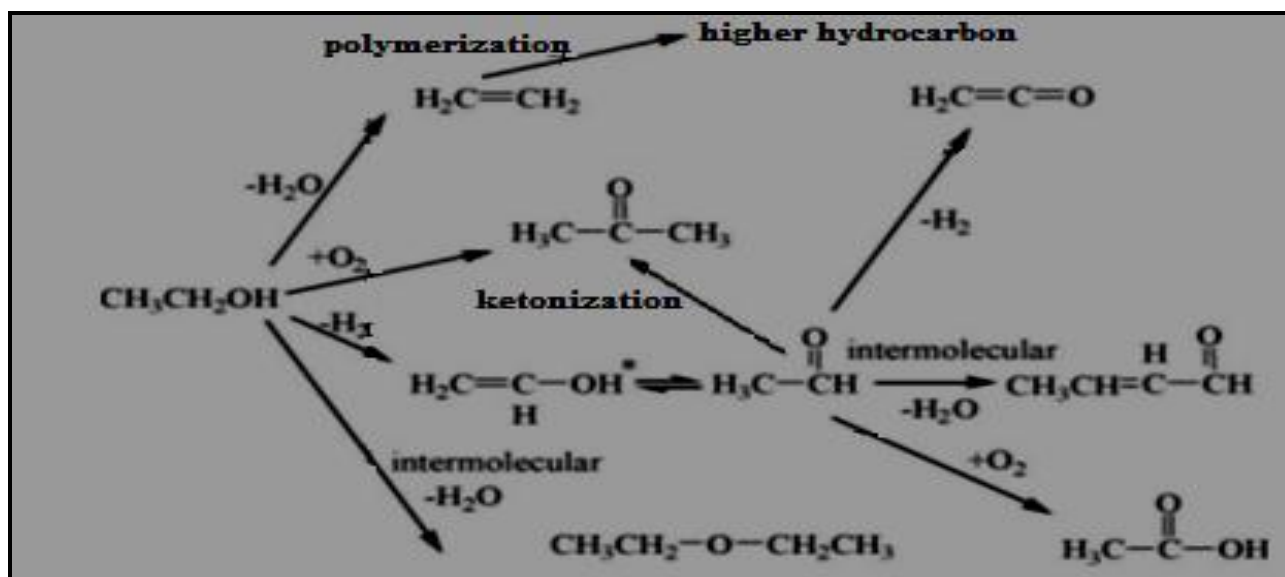
From the distribution of the converted products (Table 2), it is clear that the yield of acetone increases with the increase in the reaction temperature, and it exhibits the higher value within the reaction temperature range 100–250°C. The yield of diethylether (DEE) is slightly increased with the gradual increase in the reaction temperature from 150°C to 250°C and also low yield is obtained. Meanwhile, the yield of the heavy hydro carbon show a continuous increase.

On the other hand, the yield of ethylene and acetaldehyde are found to decrease gradually with the rising in the reaction temperature up to 250°C.

Concurrently the selectivity of the prepared graphite oxide catalyst towards the formation of the dehydrated product “ethylene” decreases with the increase in reaction temperature which goes parallel with the increase in the selectivity towards the formation of “acetone” and the oxygenated products “diethylether” and also with the decrease in the dehydrogenated product “acetaldehyde” as shown in Table 2, and histogram (Fig.9).



Scheme (1): The Suggested Pathway of the Oxidation –Reduction Reaction of Ethanol

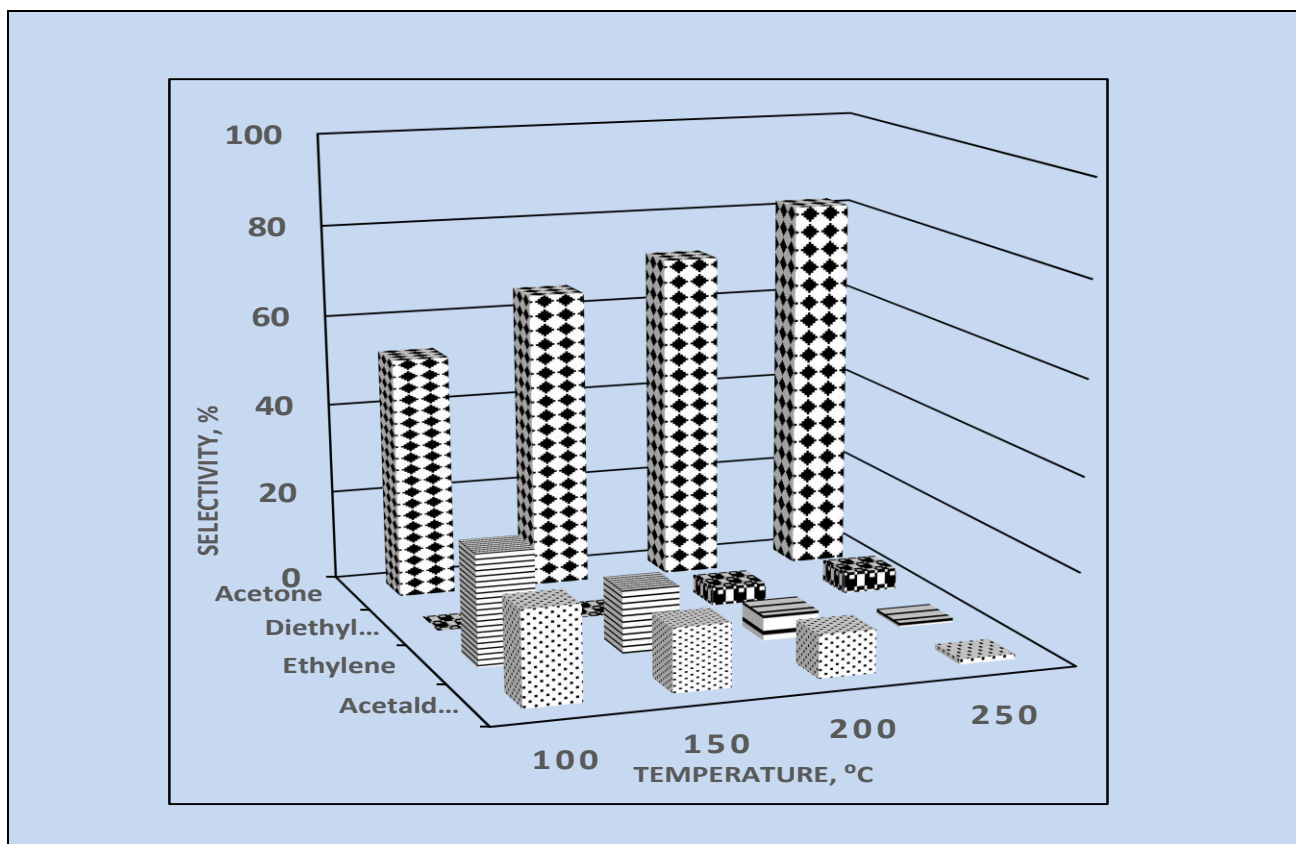


Ethanol undergoes dehydration reaction to give ethylene via intermolecular dehydration mechanism as accomplished to the presence of Brönsted acid sites. Mean while, the yield of ethylene was decreased with the increase in the reaction temperature. This may be attributed to that : under high temperature and pressure, the ethylene polymerized to the higher hydrocarbon (poly ethylene) [16]. The ethanol dimers lead to the formation of diethyl ether via bimolecular (intramolecular) dehydration reactions of ethanol catalyzed by Brönsted acid sites exposed on the catalyst surfaces[17].

Table 2: Effect of Reaction Temperature on the Catalytic Conversion of the Ethanol

Products, %	Reactiontemperature, °C			
	100	150	200	250
<b>Total Conversion</b>	14.40	37.53	56.49	91.70
A- Gaseous products	0	0.4	0.6	1.8
B- Liquid products	14.40	37.13	55.90	89.90
<b>Distribution to the Converted Liquid Products</b>				
Ethylene	3.50	5.09	3.09	0.89
Acetaldehyde	2.94	5.08	5.21	1.01
Diethylether	0.00	0.05	2.21	4.21
Acetone	7.65	24.32	40.06	73.75
Heavy hydrocarbons	0.31	2.60	5.32	10.04
<b>Selectivity to the Converted Products, %</b>				
Ethylene	24.31	13.70	5.53	1.00
Acetaldehyde	20.38	13.67	9.32	1.12
Diethylether	0	0.14	3.95	4.68
Acetone	53.13	65.50	71.67	82.04

Fig. 9: The Selectivity of the Converted Products at Different Reaction Temperature



On the other hand, acetaldehyde was produced via dehydrogenation reaction, and decreased with increasing in reaction temperature in parallel with the formation of acetone (Fig.9), confirming that, ethanol undergoes dehydrogenation reaction give acetaldehyde as an intermediate followed by aldol condensation reaction due to  $\alpha$ -H atom present in acetaldehyde to give acetone and/or dehydration to give diethyl ethers as shown in (scheme 1) .

The selectivity to acetone increased sharply with a remarkable amount with the increase in the reaction temperature until reached its maximum value (82%) at 250°C (Table 2), this may be attributed to:

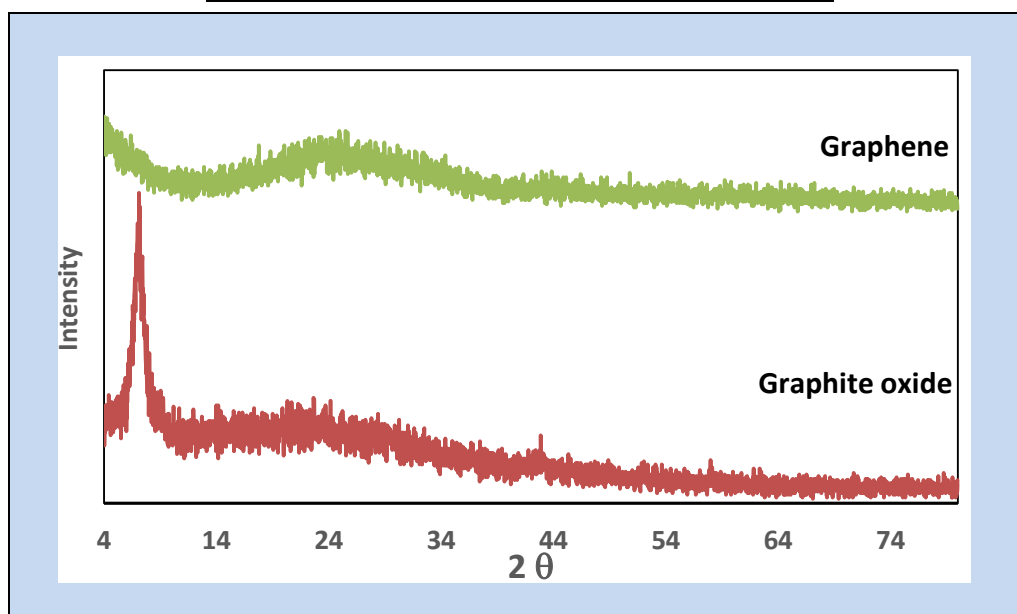
- i) The layer expansion allows the desorbated acetone through condensation/ketonization pathways to proceed easy without product diffusion hindering, as consistent with XRD data. and
- ii) The lattice defect resulting from the oxidation of graphite into graphite oxide produces different oxygen functionalities at different GO sites. Epoxy and hydroxyl groups are mainly located on the basal plane, and carbonyl, carboxyl, and esters are located at the edge and vacancy sites (as confirmed by FTIR)[18], may participate in the acetone formation reaction.

### 3.3 Characterization of the Produced Graphene

Its widely known that the graphite oxide can be converted to graphene layers with reasonable sheet resistance through thermal and/or chemical reduction treatment[19] . On using the graphite oxide as catalyst to carry out the oxidation-reduction reaction of ethanol to produce petrochemical product , the graphite oxide samples also under go reduction and exfoliation forming reduced graphene sample.

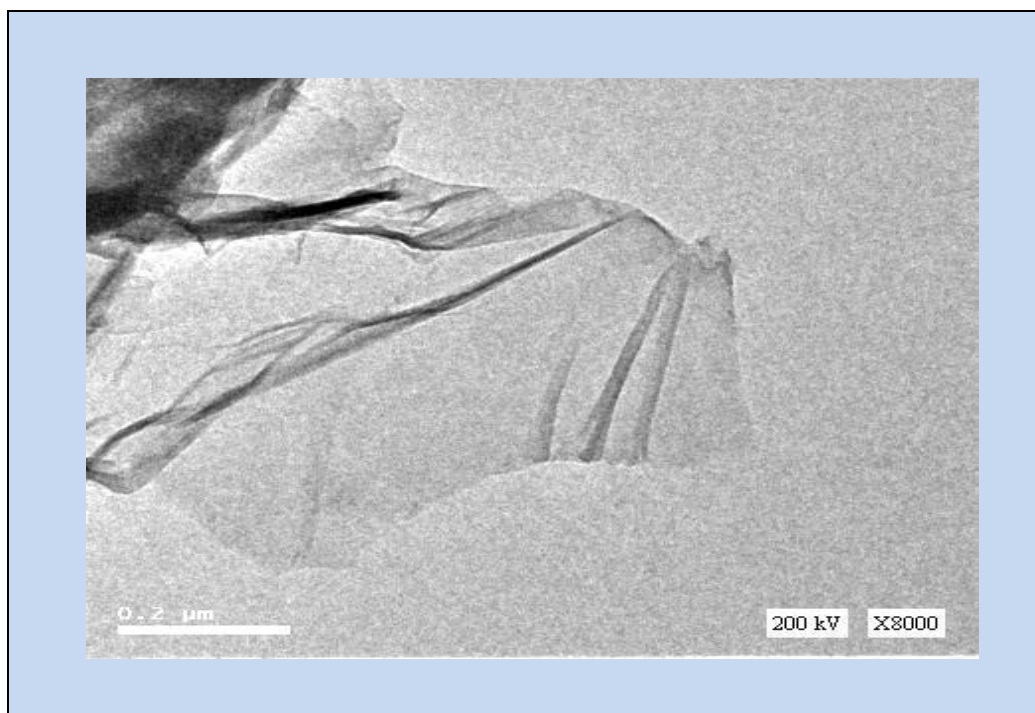
The XRD analysis of the graphite oxide and graphene (Fig. 10) indicate that the graphite oxide sample has a sharp peak at  $2\theta \sim 8^\circ$  corresponding to an interlayer distance of 0.97 nm. This interlayer distance is larger than graphitic (0.34 nm) [20], which is due to the introduction of large oxygen- functional groups in graphite oxide[21] . The diffractogram for the graphite oxide after the oxidation-thermal reaction of ethanol has attained (Fig 10), shows a broad peak centered at around  $2\theta \sim 25^\circ$  which is corresponding to the interlayer spacing of about 0.36nm., and the disappearance of the previous peak at ( $\sim 8^\circ$ ) . This means that the ethanol- thermal reaction can effectively remove the most of oxygen- functional groups and restore the conjugated network of the graphitic lattice in the reduced graphene.

Fig. 10 : XRD Pattern of the Produced Graphene



TEM image of the reduced graphene (fig.11 ) reveals the appearance of the transparent graphene sheets with wrinkle and fold features, which may created the defective structures , formed during the reduction process of graphite oxide.

Fig. 11: TEM Image of the Produced Graphene



#### 4. Conclusions

From the previous result it can be concluded that:

X-ray diffraction , Fourier transform infrared spectroscopy (FTIR) , TEM and zeta potential data ,the prepared graphite oxide consists of intact graphitic regions interspersed with sp<sup>3</sup> hybridized carbons containing hydroxyl and epoxide functional groups on the top and bottom surfaces of the sheet and sp<sup>2</sup> hybridized carbon containing carbonyl and carboxyl functional groups mostly at the sheet edges, and The optimum condition for preparing graphite oxide is 24hrs(oxidation time) and with KMnO<sub>4</sub>: Graphite of wt. ratio 3:1.

On using the best prepared graphite oxide sample as an oxidant for the oxidation – reduction reaction of ethanol .It was found that acetone is the main product with selectivity from to 82with the increase in reaction temperature from 100to 250<sup>o</sup>c .

Graphene like material was also produced (during the oxidation –reduction reaction of ethanol) i.e: the graphite oxide material was reduced to form graphene as confirmed by XRD and TEM analysis.

#### 5. Reference:

- [1] Saxena, S , Tyson ,TA.(2007) Interacting quasi-twodimensional sheets of interlinked carbon nanotubes: a high-pressure phase of carbon, ACS Nano 3515-3521
- [2] Coughlin, RW. (1967) Ind. Eng. Chem.
- [3] Song,HS, Park, MG, Ahn,W, et al., Enhanced adsorption of hydrogen sulfideand regeneration ability on the composites of zinc oxide with reduced graphite oxide, (2014) Chem. Eng. J.
- [4] Kyzas,GZ, Bikiaris, DN, EA. Deliyanni, EA, (2014) Advanced low-swelling chi-tosan/graphite oxide-based biosorbents, Mater. Lett.
- [5] Wang, HL, Kakade, BA, Tamaki,T, et al.,(2014) Synthesis of 3D graphite oxide-exfoliated carbon nanotube carbon composite and its application as catalystsupport for fuel cells, J. Power Sources .
- [6] Ubbelohde, A R, Lewis, FA, (1960) Graphite and Its Crystal Compounds, Clarendon, Oxford.
- [7] Dimiev, A., Kosynkin, DV., Alemany, LB., Chaguine, P., Tour, JM.(2012): J. Am. Chem. Soc..
- [8] Hummers'ws, Offeman RE(1958): J.AM chem soc..
- [9] carbon 50 (2012) 3497-3492.
- [10] Gudarzi, MM., Moghadam, M HM. & Sharif, F(2013):carbon .
- [11] Szabo , T, Berkesi, O, Forgo, P, Josepovits, K, Sanakis, Y, Petridis, D and Dekany I: 2006 Chem. Mater.
- [12] Jeong, H K, Jin, M.H, So, K. P, Lim, S C and Lee Y H: 2009 Tailoring the characteristics of graphite oxides by different oxidation times J. Phys. D: Appl. Phys.
- [13] Jeong, HK, Colakerol, L, Jin, M H, Glans, PA, Smith, K E and Lee, Y H 2008 Chem. Phys. Lett.
- [14] Zu, YH, Tang, J.Y, Zhu, WC, Zhang, M, Liu, G, Liu, Y Zhang, W.X. . Jia, M.J,(2011) Graphite oxide-supported CaO catalysts for transesterification of soybean oil with methanol, Bioresour. Technol.
- [15] Jeong, H K, Jin1 M H, So, K P, Lim S C and Lee Y H: (2009)J. Phys. D: Appl. Phys.
- [16] Chiang, H, Bhan, A. 2010 Catalytic consequences of hydroxyl group location on the rate and mechanism of parallel dehydration reactions of ethanol over acidic zeolites, J. Catalysis
- [17] Tullo, A.H. 2011Braskem's Push. Chem. Eng. News.
- [18] Li Z, Zhang W, Luo Y, Yang J, Hou JG. 2009 How graphene is cut upon oxidation? J Am Chem Soc .
- [19] Becerril H A, Mao J, Liu Z, Stoltenberg R M, Bao Z and Chen Y 2008 : ACS Nano
- [20] Du bin S, Gilje S, Wang K, Tung V C, ChaK, HallA S, etal. 2010 A one-step, solvothermal reduction method for producing reduced graphene oxide dispersions in organic solvents. ACS Nano
- [21] Zhu C Z, Guo S J, Fang Y X, Dong S J. 2010 Reducing sugar: new-functional molecules for the green synthesis of graphene nanosheets. ACS Nano .